International Journal of Engineering Research & Technology (IJERT)
ISSN: 2278-0181
Vol. 7 Issue 02, February-2018

Conductivity-depth Imaging of Large Loop TEM Sounding Data Acquired using Central loop Configuration

Ashish Kumar Tiwari, N. P. Singh and S. P. Maurya
Department of Geophysics, Institute of Science,
Banaras Hindu University, Varanasi, India-221005

Abstract **- A conductivity-depth imaging algorithm is developed for rapid and robust interpretation of large loop transient electromagnetic (TEM) sounding data acquired using central loop configuration. In this technique, the data obtained from the airborne or ground TEM survey, taken as the derivative of the secondary field, i.e. impulse response of secondary field and measured in form of decay voltage at successive delay times are inverted to get the conductivity depth model in an iterative least square approach. The voltage-time decay curves are transformed in from of conductivity-depth sections to represent pictorial distribution of conductivity versus depth. The technique is applied on synthetic data over homogeneous half-space (noise free and nosy data with random noise) to check the stability and robustness of the solution. The results obtained for synthetic data indicate that the algorithm is a robust one for conductivity-depth imaging of large loop TEM sounding data. Further, the techniques have been applied for inversion of large loop central loop TEM sounding data over two and three layer earth models with addition of 3% and 5% random noises. From the results, it is observed that there is good matching between the original voltage response data points and inverted voltage response curves, as well as between the final inverted models and the original models over which data were generated. The matching of inverted results with the theoretical results depicts the efficacy of the program to perform the inversion even with noisy data (with addition of 5% random noise) and of its possible application to the real field data.**

Keywords: Large loop TEM methods, TEM sounding data, Transient electromagnetic technique, Conductivity depth section, layered earth model

I. INTRODUCTION

Conductivity-depth inversion/imaging (CDI) has proven to be a useful tool in mapping the distribution of the geologic conductivity and identification of conductive sources within the variably conductive host geology. There are number of methods for deriving conductivity-depth sections from time-domain EM data ([5]; [6]; [7]; [10]; [15]; [16]), based on different approaches. Of these various conductance-depth and/ or conductivity depth imaging techniques, each one is meant for the specific case and is suitable for a particular source excitation (i.e. impulse/step/saw tooth wave etc.), survey configuration (central loop or coincident loop configuration) and is not amenable to its adoptability for commercially used other TEM systems except for the particular one for which it is developed.

Moreover, among the various transient electromagnetic (TEM) methods, the large loop TEM methods represents a class of TEM methods with large grounded transmitter loop for energizing the ground and a small receiver loop or magnetometer for recording the transient voltage or magnetic field at the center of the loop or at any arbitrary point either inside or outside the source loop. However, using a large loop source, TEM data can be acquired in any one of the configurations, namely, central loop method (with receiver at the center of the loop), in-loop method (with receiver at arbitrary in-loop point), offset loop method (with receiver at an arbitrary offset loop point in the vicinity of the source loop) and coincident loop method (with receiver loop being coincident with the source loop). Of all these configurations, the central loop system has been developed extensively and used widely for the practical surveys in the field ([3]; [7]; [8]; [9]; [11]; [13]; [14]; [17]; [18]; [19]; [20]; [21]; [22]; [23]; [24]; [25]; [27], [28]; [29]; [30];), because of the computational simplicity associated with the central loop configuration as compared to the arbitrary in-loop and offset loop configurations. In present work, an attempt is made to develop a robust conductivity-depth inversion technique capable of generating conductivity depth imaging (CDI) of TEM data acquired using large loop source (impulse excitation) and central loop configuration with provision of modification for its adaptability to TEM data acquired using commercial TEM survey configurations.

There are various techniques available in the literature for imaging of TEM measurement (voltage decay curve) time-domain central loop EM ([1]; [5]; [10]; [12]; [15]; [24]; [25]; [26]; [27]; [32]). In present research the continuous voltage versus time curve is converted into the conductivity-depth section using the concept as given in([1]). A conductivity-depth imaging algorithm is developed for the imaging of TEM sounding data acquired using central loop (large source) configuration with the provision of its adaptability to most widely used commercial TEM systems with different source excitations and survey configurations.

II. THEORETICAL BACKGROUND

In this technique the data obtained from the TEM survey (airborne TEM or ground TEM survey) is taken as the derivative of the secondary field; i.e. impulse response of the secondary field. The transmitter is considered as a loop (magnetic dipole) for airborne system and a large loop for ground and borehole system. The voltage versus delay time

International Journal of Engineering Research & Technology (IJERT)
ISSN: 2278-0181
Vol. 7 Issue 02, February-2018

curve is inverted to obtain the conductivity versus depth data in a least square sense in a manner similar to ([1]; [2]).
The plan view of large loop TEM method with central loop configuration over a layered earth is shown in Figure 1. The large loop presents a source loop and small loop at center of the source loop (P_1), represents receiver position corresponding to the central loop configuration.

In general, the data collected from a large loop TEM system consist of vertical voltage measurements made at various time intervals after the current in transmitter is turned off. These voltage measurements are related to the time derivatives of vertical magnetic field $(\partial h/\partial t)$in accordance with the following relation,

$$V(t) = -\mu_0 \left(\frac{\partial h}{\partial t}\right) M \qquad (1)$$

where *M* is the area-turns product of the receiver coil.

These voltage data can be inverted directly for the layered earth models or it can be further transformed to the apparent resistivity and then inverted. Sometime it is preferable to use apparent resistivity transformation to have a direct relation with the geo-electrical section and for getting an initial estimate of layer resistivities, which is often required for the non-linear inversion.

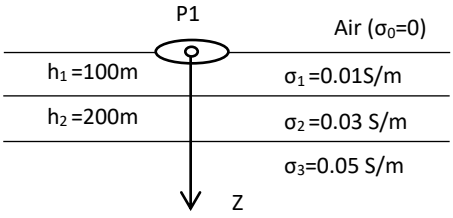

Fig. 1: Plain view of large loop central loop TEM configuration.

A. *Forward Modeling*

The forward solution for the time derivative of vertical magnetic field $(\frac{\partial h_z}{\partial t})$are obtained by transforming the frequency domain solutions for the vertical magnetic field into the time domain solutions using Fourier cosine or sine transform as given in. ([17]),

$$\frac{\partial h_z(t)}{\partial t} = \frac{-2}{\pi}\int_0^\infty Re[H_z(\omega,\rho,h)]\cos(\omega t)d\omega \qquad (2)$$

$$\frac{\partial h_z(t)}{\partial t} = \frac{2}{\pi}\int_0^\infty Im[H_z(\omega,\rho,h)]\sin(\omega t)d\omega \qquad (3)$$

where$Re[H_z(\omega,\rho,h)]$and $Im[H_z(\omega,\rho,h)]$are the real and imaginary parts of the vertical magnetic field over a layered earth in frequency domain. The component of vectors ρ and h are the resistivities and thickness of different layers of the layered earth model, and ω is the angular frequency ([10]).

The frequency domain expressions of EM field components at a point on or above the surface of an *n*-layered earth due to a finite horizontal circular loop of radius *a*, carrying a current $Ie^{i\omega t}$and placed at the height $z = -h$ above the surface of layered earth is taken from([31]).The expression of *Hz* field component at a measurement point on the surface of *n*-layered earth (i.e. at *z=0)* can be written as,

$$H_z(\omega,\rho,h) = \frac{Ia}{2}\int_0^\infty \frac{[e^{-u_0 h}(1+r_{TE})]\lambda^2}{u_0} J_1(\lambda a)J_0(\lambda r)d\lambda \quad (4)$$

where $r_{TE} = \frac{Y_0 - \hat{Y}_1}{Y_0 + \hat{Y}_1}$

with$Y_0 = \frac{u_0}{i\omega\mu_0}$ (intrinsic admittance of free space)

and$\hat{Y}_1 = \frac{H_y^{TE}}{E_x^{TE}} = -\frac{H_x^{TE}}{E_y^{TE}}$ (surface admittance at z = 0)

For an *n*-layer case, the surface admittance are given by the recurrence relation,

$$\hat{Y}_1 = Y_1\frac{\hat{Y}_2 + Y_1\tanh(u_1h_1)}{Y_1 + \hat{Y}_2\tanh(u_1h_1)} \qquad \hat{Y}_n = Y_n\frac{\hat{Y}_{n+1} + Y_n\tanh(u_nh_n)}{Y_n + \hat{Y}_{n+1}\tanh(u_nh_n)}$$

and $\hat{Y}_n = Y_n$

with $Y_n = \frac{u_n}{i\omega\mu_n}$,

$u_n = (k_x^2 + k_y^2 - k_n^2)^{1/2} = (\lambda^2 - k_n^2)^{1/2}$

and $k_n^2 = \omega^2\mu_n\varepsilon_n - i\omega\mu_n\sigma_n$

Here, *r* is source-receiver offset (measured from center of the loop). For calculation purposes, $\tanh(u_nh_n)$ is used in its exponential form for stability reasons ([12]).

Therefore, starting with computation of $H_z(\omega,\rho,h)$field (equation 4), using the method described in ([26]), we have computed the time derivative of vertical magnetic field using the Fourier cosine and sine transforms (equations 2 and 3) ([26]; [32]). Thereafter, we have computed the voltage response which is needed as forward computation in this inversion scheme.

B. *Inversion (Imaging) Approach*

In general, for solving the TEM non-linear inverse problems, there exist two approaches. The first is to make no assumption about the conductivity distribution in the earth and find the classes of conductivity models that fit the data, like Occam's inversion used in([7]). The second approach, which is more practical in many exploration problems, is to assume an initial model, representative of the earth under the consideration. Thereafter, the model parameters are estimated using an optimization technique. The important aspect of the second approach is the assumption of correct class of model. This approach allows for geological and geophysical information to be incorporated into the inverse problems. The major disadvantage of this approach is that by assuming an initial model, there is always a chance of unknown bias introduced into the inverse problem ([8]).

In present research, we have followed the second approach, i.e. model fitting approach, where the initial model is the layer earth with parameters consisting of resistivities and thicknesses of different layers. For the inversion, we have followed ([1]) approach with some modification in scheme and changes in input parameters in accordance with need of the present problem and to overcome the practical limitations associated with the NLSTCI program for the central loop case. The NLSTCI program is modification of a general nonlinear least square algorithm of ([4]) to that of a constrained and unconstrained algorithm with weighted observations, and is more reliable than a Gauss-Newton or Leven berg-Marquardt algorithm when a large residual exists between data and forward solution. To overcome the problem of local minima

International Journal of Engineering Research & Technology (IJERT)
ISSN: 2278-0181
Vol. 7 Issue 02, February-2018

associated with NLSTCI, in our program, we have made some adjustment in the program that in next step it recalls the program by replacing initial model parameters with inverted parameters obtained in the previous step and repeat the process for the desired number of steps or till it get a reasonable model parameters. This is achieved through the use of the fact that at each step program start with new value of A (Marquardt parameter) depending upon the resulting residual at that step and some special procedures. The forward problem is based on ([24]),which is entirely different to that in ([1])program, which uses ([2])algorithm for computation of central loop frequency domain response. The inversion is based on minimization of a residual misfit function in an iterative least square process. The misfit function, which is minimized in an iterative process, can be defined as following.

$$V(F) = \frac{1}{2}[V(RNORM)]^2 \quad (5)$$

$$V(RNORM) = \frac{1}{\sqrt{n}}\sum_{i=1}^{n} R(I) \quad (6)$$

$$R(I) = SQWT(I) * (Y(I) - F) \quad (7)$$

$$SQWT(I) = sqrt\big(WT(I)\big) \quad (8)$$

where *Y(I)* and *WT(I)* are the Ith data point and corresponding weight factor, and *F* is corresponding calculated value.

III. RESULTS AND DISCUSSIONS

For checking the accuracy and efficiency of the program for inverting the large loop TEM data, we have applied it for the inversion of large loop TEM data acquired using central loop configurations over the homogeneous, two layer and3-layer earth models. The inversion is tested for the noise free as well as for the noisy data (with addition of random noise), and some relevant results are shown in Figures 2-7.

Figure 2 presents inversion results for the large loop TEM data over the homogeneous earth model with 5% random (Gaussian)noise for central loop TEM configuration and source loop of radius 50 m. The data points and inverted voltage response curve are shown by open circles and dotted curves in Figure 2(a), whereas the original model for which data was generated and the final inverted model are shown in Figure 2(b). The inversion was stared with an initial homogeneous model of conductivity 0.001 *S/m* for noise free, 1% random noise, 3% random noise and 5% random noise but only 5% inversion results are shown in this paper. From Figure 2(a), it is observed that there is good matching between the original data points and inverted voltage response data. Figure 2(b) depicts that final inverted model is in good agreement with the original model with which data was generated. The conductivity of homogeneous layer is reproduced with difference as little as 0.01%.

Figure 3 shows inversion results for the voltage response data over the 2-layer earth model without noise for the central loop system and source loop of radius 50 m. Figure 3(a) shows data points and inverted voltage response curve, while Figure 3(b) shows original and final inverted2-layer models. The initial model with which inversion was started is a homogeneous model with conductivity 0.001 *S/m*. Figure 3(a) depicts that there is good agreement between the observed and inverted voltage response data leading to the final model as shown in Figure 3(b). From Figure 3(b), it is observed that the inverted model is in agreement with the original synthetic model with which data was generated.

Figure 4 depicts inversion results for large loop TEM voltage response data over the 2-1ayerearth model for the central-loop configuration with 3% random noise. The radius of source loop is 50 m and the receiver loop lies at center of the loop. Figure 4(a) shows data points and inverted voltage response, and Figure 4(b) shows original and inverted2-layer earth models. The inversion was started with a homogeneous model of conductivity 0.001 *S/m*. From Figure 4(a) it is clear that there is good agreement between the observed and inverted voltage response data, resulting in a final model as shown in Figure 4(b). From Figure 4(b), it is clear that the inverted model is in good agreement with the original synthetic model. The inverted parameters are recovered with significantly high accuracy, i.e. conductivities and thickness of different layers interpreted from inversion indicates that there is an average variation of less than 0.1%.

Figure 5 shows inversion results for the large loop TEM voltage response data over the 2-layer earth model for the central loop configuration with 5%random noise. The source loop radius is 50 m. Figure 5(a) shows the original data points and the inverted voltage response curves, and depicts that there is good matching between the original data points and inverted curve. Figure 5(b) shows original and inverted 2-layer models. The inversion was started with a homogeneous model of conductivity 0.001S/m. Figure 5(b) depicts that there is good agreement between the inverted and original model with which data was generated. The inverted parameters, i.e. conductivities and thickness of different layers are close to the original parameters. The average variation of inverted parameters is less than 1%. These results depict accuracy and capability of the method for inversion of large loop TEM data acquired using central loop configuration. Further, the inversion was carried out for more than 5% Gaussian noise in the data and it is noticed that the inversion algorithm does not work properly and gives ambiguous results.

Thereafter, the algorithm is further applied for inverting the voltage time data over a 3 layer (as in Figure 1) with addition of 1%, 3%, 5% and more than 5% random noises. However, only noise free and 5% random noise data results are shown. Figure 6 shows inversion results for the large loop TEM voltage response data over the 3-layer earth model for central loop configuration for noise free data. The loop radius is 50 m. Figure 6(a) shows data points and inverted voltage response curves which depicts that there is good matching between the data points and inverted curve. Figure 6(b) shows original and inverted 3-layer models. The inversion was started with a homogeneous model of conductivity 0.001S/m. Figure 6(b), depicts that there is good agreement between the inverted and original model with which data was generated. The inverted parameters, i.e. conductivities and thicknesses of different layers are close to the original parameters. The average variation of inverted parameters is less than 3%. These results depict accuracy and capability of the method for inversion of large loop TEM data over 3layer earth models acquired using central loop configuration.

International Journal of Engineering Research & Technology (IJERT)
ISSN: 2278-0181
Vol. 7 Issue 02, February-2018

Figure 7 shows inversion results for the large loop TEM voltage response data over the 3-layer earth model for central loop configuration with 5%random noise and the source loop radius as 50 m. Figure 7(a) shows original data points and inverted voltage response curve, which depicts that there is good matching between the data points and inverted curve. Figure 7(b) shows original and inverted 3-layer models. The inversion was started with a homogeneous model of conductivity 0.001S/m. Figure 7(b), depicts that there is good agreement between the inverted and original model with which data was generated. The inverted parameters, i.e. conductivities and thicknesses of different layers are close to the original parameters. The average variation of inverted parameters is less than 5%. These results depict accuracy and capability of the method for inversion of large loop TEM data acquired using central loop configuration over the 3 layer earth models. Further, the inversion is carried out for the more than 5% Gaussian noise in the data and it is noticed that the inversion algorithm is not working properly and giving ambiguous results.

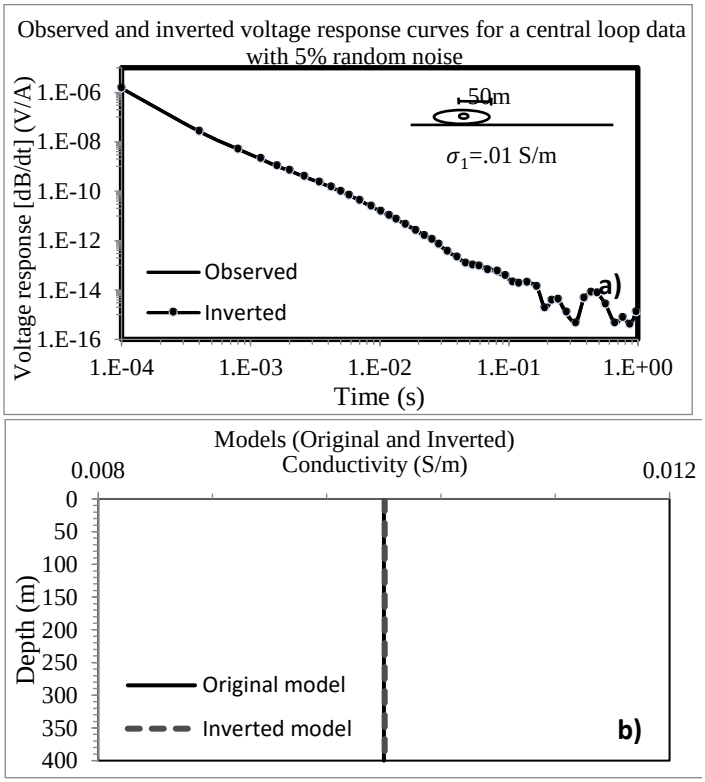

Fig 2: Inversion results for the large loop central loop TEM data with loop radius 50m over a homogeneous earth model with 5% random noise, (a) The synthetic data points and inverted best fit curves, (b) The original model with which data was generated and the final inverted model obtained after the inversion.

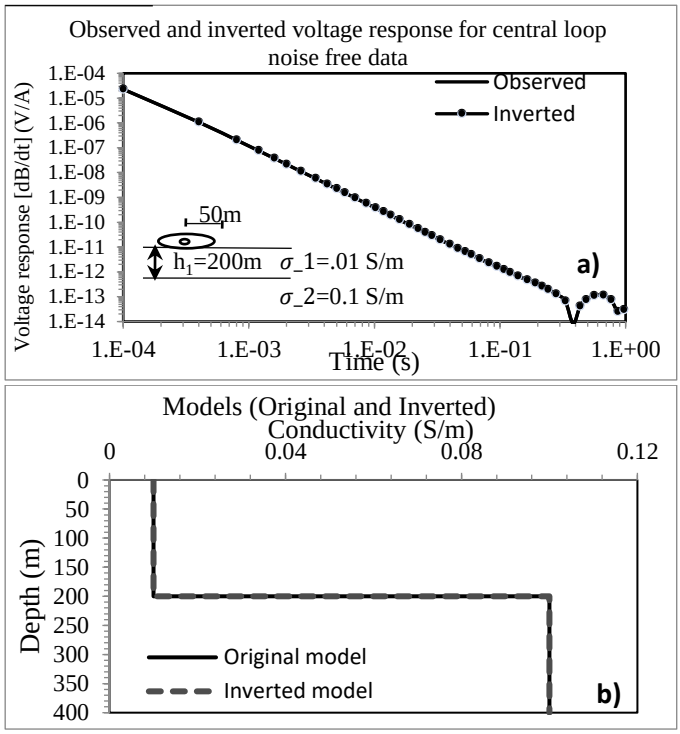

Fig 3: Inversion results for the large loop central loop TEM voltage response noise free data over 2 layer earth model with source loop radius 50m, (a) The synthetic data and best fit curves, (b) The original model with which data was generated and the final inverted model obtained after inversion.

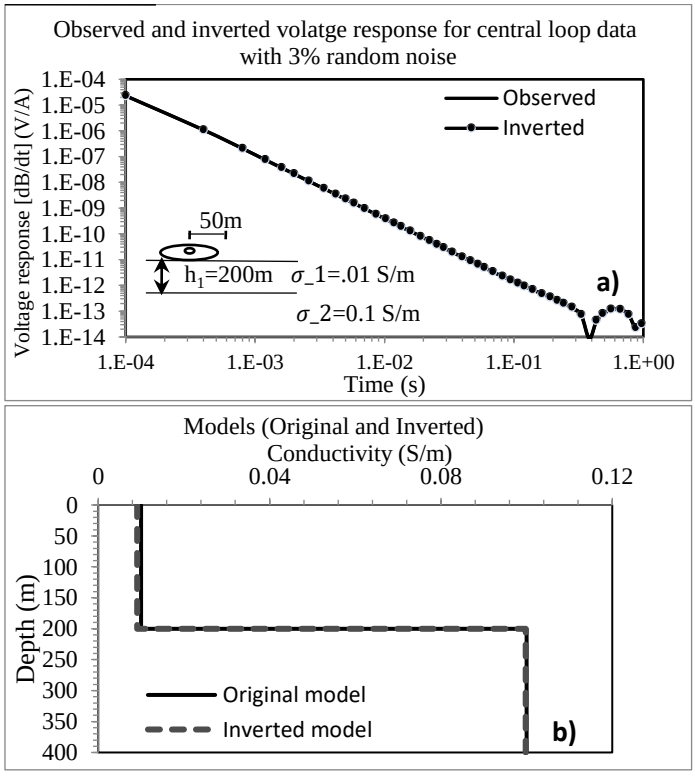

Fig 4: Inversion results for the large loop central loop TEM data with source loop radius 50m over a 2 layer earth model with 3% random noise. (a) The synthetic and best fit curves, (b) The original model with which data was generated and the final inverted model obtained after inversion.

International Journal of Engineering Research & Technology (IJERT)
ISSN: 2278-0181
Vol. 7 Issue 02, February-2018

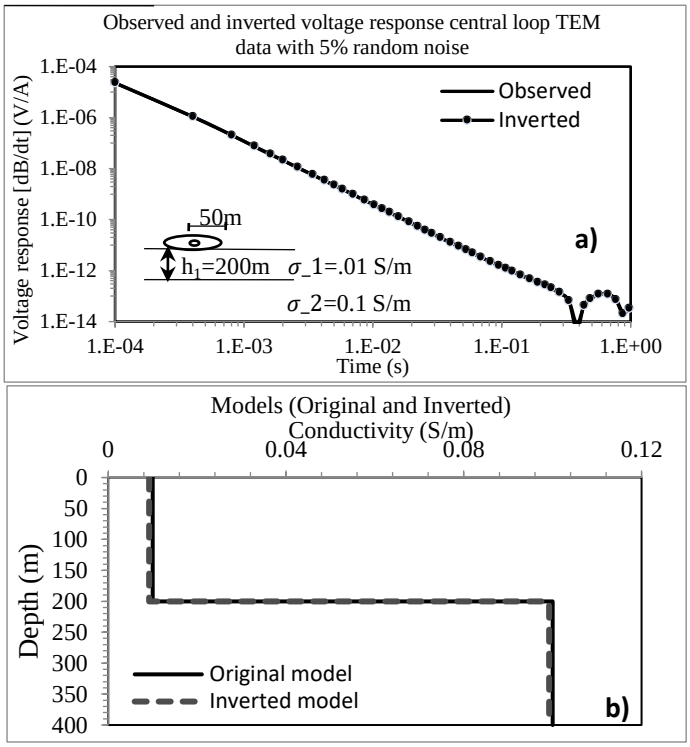

Fig 5: Inversion results for the large loop central loop TEM data with loop radius 50m over a 2 layer earth model with 5% random noise. (a) The synthetic and best fit curves, (b) The original model with which data was generated and the final inverted model obtained after inversion.

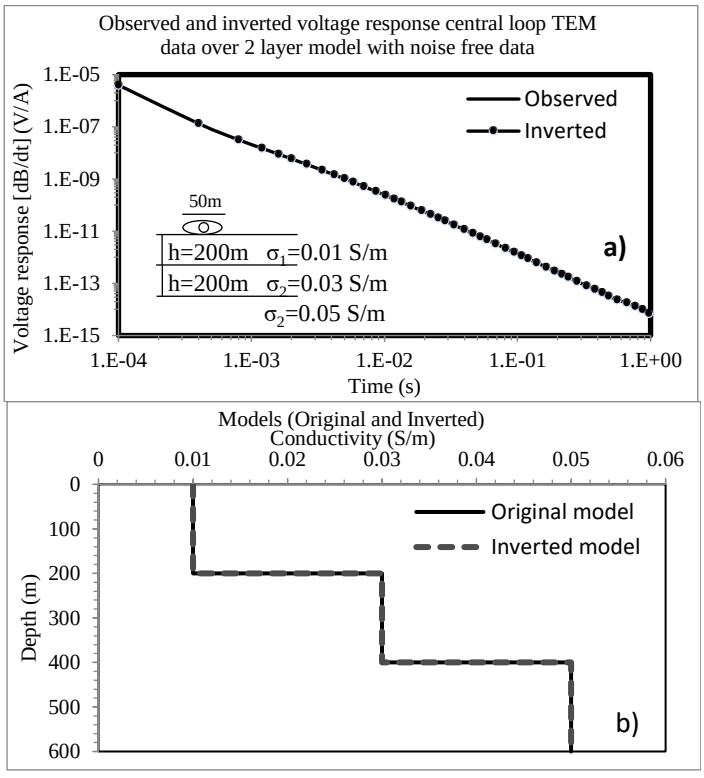

Fig.6: Inversion results for the large loop central loop TEM noise free data with loop radius 50m over 3 layer earth model, (a) The synthetic and best fit data curves, (b) The original model with which data was generated and the final inverted model obtained after the inversion.

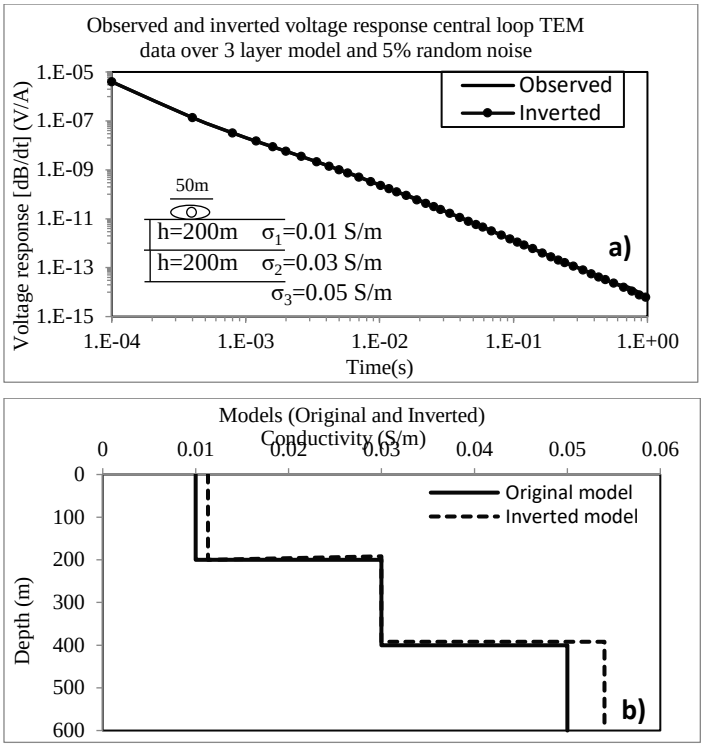

Fig 7: Inversion results for the large loop central loop TEM data with loop radius 50m over 3 layer earth model with 5% random noise, (a) The synthetic and best fit data curves, (b) The original model with which data was generated and the final inversion model obtained after inversion.

IV. CONCLUSION

A conductivity-depth imaging algorithm is developed for the rapid and robust interpretation of large loop TEM sounding data acquired using central loop configuration. For checking the stability and robustness of the algorithm, it is applied on the synthetic data over homogeneous half-space, 2 layer and 3 layer models with and/or without addition of random noises. The analysis shows that the inverted results match nicely with the original model result for all the cases, which indicate that the developed algorithm is very robust and gives stable solution for inversion of large loop TEM sounding data over the layered earth models. The results depicts efficacy of the program to perform inversion even with the noisy data and its possible use for the inversion of real field large loop TEM data.

ACKNOWLEDGMENT

One of the authors (AKT)is thankful to the Department of Geophysics, Banaras Hindu University, Varanasi for giving opportunity and facility for completion of this work.

REFERENCES

[1] Anderson, W.L., Nonlinear least-squares inversion of transient soundings for a central induction loop system (Program NLSTCI), US Geological Survey, 1982, pp. 30.

[2] Anderson, WL , Numerical integration of related Hankel transforms of orders 0 and 1 by adaptive digital filtering, Geophysics, 1979, vol. 44(7), pp.1287-1305.

[3] Buselli G., Barber C., Davis G. B. and Salama R.B., Detection of groundwater contamination near waste disposal sites with transient electromagnetic and electrical methods, Geotechnical and Environmental Geophysics, 1990, vol. 2, pp.27-39.

[4] Dennis, J., Gay, D. and Welsch, R., An adaptive non linear least square algorithm, ACM Transaction on Mathematical Software, 1981, vol. 7(3), 348-368.

International Journal of Engineering Research & Technology (IJERT)
ISSN: 2278-0181
Vol. 7 Issue 02, February-2018

[5] Eaton, Perry A. and Gerald W.H., A rapid inversion technique for transient electromagnetic soundings, Physics of the Earth and Planetary Interiors,1989, vol. 53(3-4), pp.384-404.
[6] Fraser D.C., Resistivity mapping with an airborne multicoil electromagnetic system, Geophysics, 1978, vol. 43(1), pp.144-172.
[7] Fullagar P. K., Generation of conductivity-depth pseudo-sections from coincident loop and in-loop TEM data, Exploration Geophysics, 1989, vol. 20(1/2), pp. 43-45.
[8] Hoekstra, Pieter and Mark W. B., Case histories of time-domain electromagnetic soundings in environmental geophysics, Geotechnical and Environmental Geophysics, 1990, vol. 2, pp.1-15.
[9] Hoversten G.M. and Morrison H.F., Transient fields of a current loop source above a layered earth, Geophysics, 1982, vol. 47(7), pp.1068-1077.
[10] Huang H. and Palacky G. J., Damped Least-Squares Inversion Of Time-Domain Airborne EM Data Based On Singular Value Decomposition, Geophysical Prospecting, 1991, vol. 39(6), pp.827-844.
[11] Kaufman, Alexander A., Harmonic and transient fields on the surface of a two-layer medium, Geophysics, 1979, vol. 44(7), pp.1208-1217.
[12] Knight, J.H. and Raiche, A.P., 1982. Transient electromagnetic calculations using the Gaver-Stehfest inverse Laplace transform method. Geophysics, 47(1), pp.47-50.
[13] Lee T. and Lewis R., Transient EM response of a large loop on a layered ground, Geophysical Prospecting, 1974, vol. 22(3), pp.430-444.
[14] Liu, Guimin, and Michael A., Conductance-depth imaging of airborne TEM data, Exploration Geophysics, 1993, vol. 24(3/4), pp.655-662.
[15] Macnae J., Andrew K., Ned S., Alex O., and Andrej B., Fast AEM data processing and inversion, Exploration Geophysics, 1998, vol. 29(1/2), pp. 163-169.
[16] Macnae J., Richard S., Polzer B. D., Yves L., and Klinkert P.S., Conductivity-depth imaging of airborne electromagnetic step-response data, Geophysics, 1991, vol. 56(1), pp.102-114.
[17] Morrison H.F., Phillips R. J. and O'brien D. P., Quantitative interpretation of transient electromagnetic fields over a layered half space, Geophysical Prospecting, 1969, vol. 17(1), pp.82-101.
[18] Nabighian M.N., Electromagnetic Methods in Applied Geophysics, Society of Exploration Geophysicists, 1991, vol. 2.
[19] Nabighian M.N., Quasi-static transient response of a conducting half-space - An approximate representation, Geophysics, 1979, vol. 44(10), pp.1700-1705.
[20] Newman, G.A., Anderson, W.L. and Hohmann, G.W., 1987. Interpretation of transient electromagnetic soundings over three-dimensional structures for the central-loop configuration. Geophysical Journal International, 89(3), pp.889-914.
[21] Newman, Gregory A., Walter L.A. and Gerald W. H., Interpretation of transient electromagnetic soundings over three-dimensional structures for the central-loop configuration, Geophysical Journal International, 1987, vol. 89(3), pp. 889-914.
[22] Patra H. P., Central Frequency Sounding In Shallow Engineering And Hydro-Geological Problems, Geophysical Prospecting, 1970, vol. 18(2), pp.236-254.
[23] Rai S.S. and Sharma G.S., In-loop pulse EM response of a stratified earth, Geophysical prospecting, 1986, vol. 34(2), pp. 232-239.
[24] Singh N.P., Mitsuru U. and Tsuneomi K., TEM response of a large loop source over a homogeneous earth model: A generalized expression for arbitrary source-receiver offsets, Pure and Applied Geophysics, 2009, vol. 166(12), pp. 2037-2058.
[25] Singh, N.P. and Mogi, T., 2003. EMLCLLER—A program for computing the EM response of a large loop source over a layered earth model. Computers & geosciences, 29(10), pp.1301-1307.
[26] Singh, N.P. and Mogi, T., 2005. Electromagnetic response of a large circular loop source on a layered earth: A new computation method. Pure and Applied Geophysics, 162(1), pp.181-200.
[27] Smith, Richard S. and West G.F., An explanation of abnormal TEM responses: coincident-loop negatives, and the loop effect, Exploration Geophysics, 1988, vol. 19(3), pp.435-446.
[28] Smith, Richard S. and West G.F., Field examples of negative coincident-loop transient electromagnetic responses modeled with polarizable half-planes, Geophysics, 1989, vol. 54(11), pp.1491-1498.
[29] Spies B.R. and Raiche A.P., Calculation of apparent conductivity for the transient electromagnetic (coincident loop) method using an HP-67 calculator, Geophysics, 1980, vol. 45(7), pp. 1197-1204.
[30] Verma R.K. and Mallick K., Detectability of intermediate conductive and resistive layers by time-domain electromagnetic sounding, Geophysics, 1979, vol. 44(11), pp.1862-1878.
[31] Ward, S.H. and Hohmann, G.W., 1988. Electromagnetic theory for geophysical applications. Electromagnetic Methods in Applied Geophysics, Volume 1- Theory, (ed. M.N.Nabighian), pp.131-311, Society of Exploration Geophysicists, Tulsa, Oklahoma.
[32] Zhdanov M.S., Dmitriy A.P. and Robert G.E., Localized S-inversion of time-domain electromagnetic data, Geophysics, 2002, vol. 67(4), pp.1115-1125.